
This is an electronic reprint of the original article.
This reprint may differ from the original in pagination and typographic detail.

Khan, Yaseen; Marin, Minna; Viinikainen, Tiia; Lehtonen, Juha; Puurunen, Riikka L.; Karinen, Reetta

Structured microreactor with gold and palladium on titania

Published in:
Applied Catalysis A: General

DOI:
[10.1016/j.apcata.2018.06.010](https://doi.org/10.1016/j.apcata.2018.06.010)

Published: 25/07/2018

Document Version
Peer-reviewed accepted author manuscript, also known as Final accepted manuscript or Post-print

Published under the following license:
CC BY-NC-ND

Please cite the original version:
Khan, Y., Marin, M., Viinikainen, T., Lehtonen, J., Puurunen, R. L., & Karinen, R. (2018). Structured microreactor with gold and palladium on titania: Active, regenerable and durable catalyst coatings for the gas-phase partial oxidation of 1-butanol. *Applied Catalysis A: General*, 562, 173-183. <https://doi.org/10.1016/j.apcata.2018.06.010>

This material is protected by copyright and other intellectual property rights, and duplication or sale of all or part of any of the repository collections is not permitted, except that material may be duplicated by you for your research use or educational purposes in electronic or print form. You must obtain permission for any other use. Electronic or print copies may not be offered, whether for sale or otherwise to anyone who is not an authorised user.

Structured microreactor with gold and palladium on titania: active, regenerable and durable catalyst coatings for the gas-phase partial oxidation of 1-butanol

Yaseen Khan^{a+*}, Minna Marin^{a+}, Tiia Viinikainen^a, Juha Lehtonen^{a,b}, Riikka L. Puurunen^a, Reetta Karinen^a

^a Aalto University, Department of Chemical and Metallurgical Engineering, P.O. Box 16100, FI-00076 Aalto, Finland

^b VTT Technical Research Centre of Finland, P.O. Box 1000, FI-02044 VTT, Finland

⁺ Both authors contributed equally to this work.

^{*} Corresponding author: yaseen.khan@aalto.fi

Abstract

Structured microreactors coated with catalytically active porous layers have emerged as a promising replacement for conventional reactors because they are inherently safe to operate in nearly isothermal conditions within the kinetic regime. Bio-based 1-butanol is commonly produced by acetone-butanol-ethanol (ABE) fermentation and is considered an important platform chemical that will benefit in the share of value-added chemicals through the development of new catalytic processes. In this study, monometallic gold (Au) and palladium (Pd), as well as bimetallic Au-Pd nanoparticles, supported on titania (TiO₂) were prepared by a sol-immobilization method, characterized, coated on structured microreactor plates and tested for their catalytic activity in the gas-phase partial oxidation of 1-butanol to *n*-butyraldehyde. A customized structured catalyst testing microreactor was used. The average noble metal particle size for the catalyst coatings was determined to be approximately 3.6 nm for Au and Au-Pd catalysts, and the noble metal nanoparticles were evenly distributed. The catalyst coating was 17±7 μm in thickness. The studied coated catalysts (TiO₂, Au/TiO₂, Pd/TiO₂, and Au-Pd/TiO₂) were all active for the partial oxidation of 1-butanol. The Au/TiO₂ (0.6 wt%) catalyst showed the highest yield (20%) of *n*-butyraldehyde at 300 °C. The introduction of Pd onto Au/TiO₂ or TiO₂ shifted the product distribution at 250 °C towards retro-hydroformylation and oxidation products (propene, carbon monoxide and carbon dioxide). All of the coated catalysts that were tested were mechanically stable. The nano Au/TiO₂ could be regenerated in situ and showed reproducible activities and yields in over 50 test runs. Structured microreactors coated with gold nanoparticles supported on titania show promise as a reusable and mechanically stable device for the process development of *n*-butyraldehyde production in ABE fermentation plants.

Keywords:

Bio 1-butanol, partial oxidation, *n*-butyraldehyde, heterogeneous catalyst, nanogold, titania, coated microreactors

1. Introduction

Microreactors are discussed in the literature for their potential in process intensification and for their use in kinetic studies [1,2]. Microreactors can have different configurations, such as multiple channels that can be considered together as single reactors. The channels must have at least one dimension below the millimeter range [3]. Microreactors are well known for their efficient heat and mass transfer properties. Thus, even highly exothermic reactions can be operated nearly isothermally in microreactors [3–7]. To be used in heterogeneously catalyzed reactions, the catalytically active material can be coated onto the microreactor walls [6–8]. A thin catalyst layer (<40 μm) coated on the channel walls allows an investigation of the intrinsic kinetics of the catalyst because the short diffusion lengths in the porous catalyst layer suppress any mass transfer limitations [5,9–11]. The most important parameters in using these coated plates as catalysts are the mechanical stability of the coating and its adhesion to the plates [8]. In addition, the plate material should also be able to withstand the high temperatures and pressures used in industrial applications.

In principle, microreactors could be used downstream in an acetone-butanol-ethanol (ABE) fermentation plant, where one of the products of ABE fermentation is bio-based 1-butanol [12,13]. 1-Butanol can be applied as a bio-component in traffic fuels, but it is also a platform chemical for the synthesis of many fine and specialty chemicals, which makes bio-based 1-butanol an environmentally interesting starting material [13,14]. The synthesis of aldehydes, ketones and carboxylic acids by partial oxidation reactions is of great industrial importance. Air, or pure oxygen, is a clean reagent suitable for bulk-scale oxidation reactions in both the aqueous and gas phases [15]. To avoid total oxidation products, the molar ratio of alcohol to oxygen is stoichiometrically adjusted to perform only partial oxidation reactions, and the selectivity can be further guided by using suitable catalysts [15]. Butyraldehyde, among other aldehydes, is an important molecule in the production of many high-value chemicals, as discussed in a review by Mascall [14]. Converting bio-based butanol into butyraldehyde could increase the share of renewable chemicals. Currently, butyraldehyde is produced from propene via hydroformylation, i.e., oxo-synthesis [16]. This homogeneously catalyzed process takes place at pressures of 2-35 MPa over metal carbonyl complexes [16]. The development of selective, heterogeneously catalyzed processes that work under milder conditions according to the principles of green chemistry would be both economical and enhance the on-site safety of this synthesis [17].

Recent advances in the selective oxidation of alcohols over supported gold nanoparticles (NPs) were reviewed by Sharma et al. [18]. The development of environmentally friendly and sustainable methods for the oxidation of alcohols is important for many chemical industries. The use of Au NPs for the oxidation of aliphatic and aromatic primary alcohols has drawn interest due to the ability of gold to dissociate molecular oxygen and its nontoxicity [18]. Moreover, supported Au NPs offer the opportunity for base-free and solvent-free oxidation reactions using oxygen or air to perform the reactions under moderate conditions [15]. However, the recyclability of these catalysts still remains a challenge in terms of both the number of cycles and ex situ regeneration procedures (filtration, centrifugation or magnetic separation) [18]. The activity of Au NPs depends strongly on their particle size and shape, as well as the nature of the support [18,19]. The most active Au NPs are under approximately 5 nm [18]. Moreover, supported bimetallic Au-Pd catalysts have recently been studied for the partial oxidation of primary

alcohols [20]. The different morphologies (alloy, core-shell, decorated particles) obtained for Au-Pd catalysts have been reported to have a clear correlation to their activity [21]. Thus, the properties of supported Au or Au-Pd catalysts depend heavily on the preparation method used.

The most common synthesis methods for the preparation of supported Au NPs on metal oxide supports are impregnation, deposition-precipitation and sol-immobilization [18,22,23]. The same synthesis methods can be applied to supported bimetallic Au-Pd catalysts, where metals can be incorporated either simultaneously or successively [24]. The sol-immobilization method, i.e., the colloidal method, uses organic ligands or polymers to stabilize the colloids [25]. The most common stabilizer for supported Au-Pd nanoparticles (Au-Pd NPs) is polyvinyl alcohol (PVA) [21]. The colloidal method is advantageous because the metal NPs can be synthesized with a narrow particle size distribution, and in the case of bimetallic catalysts, even the morphology can be tuned [22]. As an example, Dimitratos et al. [23] compared impregnated and sol-immobilized Au-Pd/TiO₂. The highest activity for the oxidation of glycerol was achieved with the sol-immobilized materials. However, in the partial oxidation of 1-butanol in the liquid phase, a similar sol-immobilized Au-Pd/TiO₂ catalyst resulted in a high yield of butanoic acid instead of butyraldehyde [26]. In the gas phase, the partial oxidation of primary alcohols in the presence Au catalysts seems to favor the formation of the corresponding aldehyde [15], as was recently demonstrated by Holz et al. [27] using Au/TiO₂ for the partial oxidation of ethanol. Similarly, Cu and Ru catalysts showed good yields of butyraldehyde in the gas phase [17,28]. Therefore, based on the literature, it seems that partial oxidation of 1-butanol to butyraldehyde with high yields can also be expected in the gas phase over supported Au or Au-Pd catalysts.

For heterogeneous catalysts, the choice of a support material is essential. Among many different oxide supports, titanium oxide (titania, TiO₂) is known to be chemically stable and enable strong support-metal interactions (SMSI) [29,30]. For example, a direct correlation between catalytic activity and electron transfer from the Au particles (particle sizes less than 5 nm) to the TiO₂ support was discovered by Okazaki et al. [31]. The specific surface area of titania is high. It also has a mesoporous structure and high thermal and mechanical stabilities, making TiO₂ a common heterogeneous support material [32]. The applicability of titania has already been widely demonstrated for both photocatalytic applications [33] and as a support for metal nanoparticles (NPs) in many oxidation and reduction reactions [20,23,27].

This work aimed to develop active, mechanically stable and durable coated catalysts of mono- and bimetallic Au and Pd supported on TiO₂ for the gas-phase partial oxidation of 1-butanol to *n*-butyraldehyde. A structured microreactor with the catalyst coated on the channel walls was applied in order to take advantage of rapid mass transfer and operate under isothermal conditions. Furthermore, the aim was to prepare coated catalysts with a narrow average metal particle size distribution (<5 nm) and a thin coating (<40 μm). To our knowledge, the partial oxidation of 1-butanol in the gas phase using air or oxygen over Au/TiO₂ or Au-Pd/TiO₂ coated catalysts that were prepared by a colloidal method has not been reported to date.

2. Experimental

2.1 Preparation of catalyst powders and coating of the microreactor plates

Catalyst powders were prepared via a sol-immobilization method that was modified from the procedure reported by Lopez-Sanchez et al. [22]. Fig. 1 illustrates the catalyst preparation steps, with amounts, for the 0.6 wt% Au/TiO₂ catalyst. First, polyvinyl alcohol (PVA) (80% hydrolyzed, weight average molecular weight $M_w = 9\,000\text{--}10\,000\text{ g}\cdot\text{mol}^{-1}$, Aldrich) was mixed with water for 10 minutes to achieve a 1 wt% solution. The metal precursors were a gold(III) chloride solution (HAuCl₄, Aldrich, Au conc. 30 wt% in dilute HCl) and/or palladium(II) chloride solution (PdCl₂, Alfa Aesar, Pd 20 – 25% wt/wt), which were added to a beaker. Water was then added to a total volume of 800 ml. The PVA solution (targeted PVA/metal=2 based on weight) and a 0.1 M freshly prepared solution of the reducing agent NaBH₄ (Aldrich, targeted $n(\text{NaBH}_4)/n(\text{metal})=6$) were added and mixed for 30 min. Then, the support (titanium(IV)oxide, anatase, <25 nm, 99.7% purity, Aldrich) was added and the pH was adjusted to 2-3 with sulfuric acid (H₂SO₄, 99.99%, Aldrich). This mixture was stirred for 2 h and then filtered and washed thoroughly with distilled water. The prepared catalyst powders were dried overnight at 110 °C. In a batch, 1 or 2 g of catalyst powder was prepared with the desired metal loading of 0.3 to 0.6 wt%.

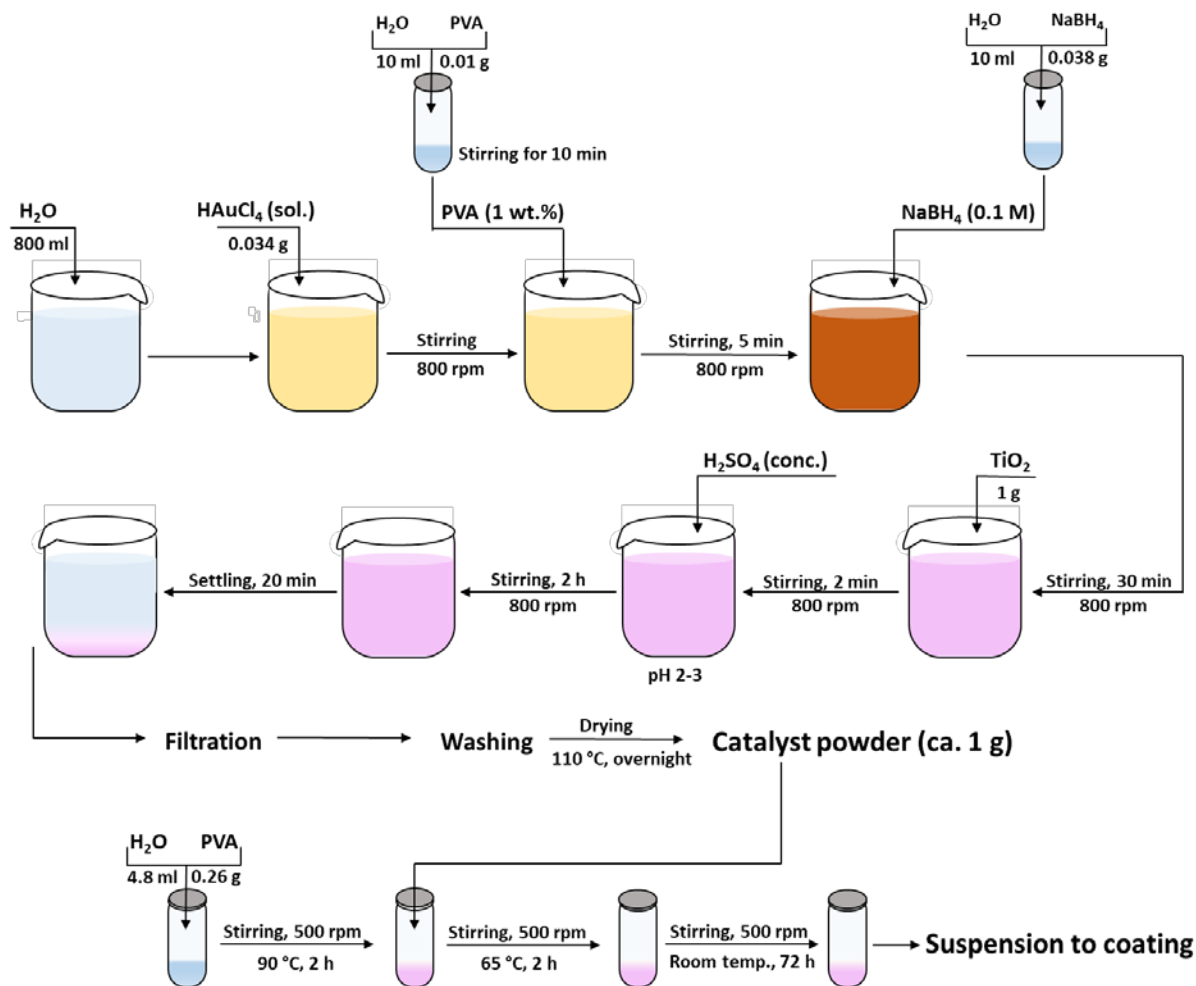


Fig. 1. Schematic of the catalyst preparation (quantities denoted for 0.6 wt% Au/TiO₂) by a sol-immobilization method for the preparation of the catalyst coating suspension.

The targeted amount (wt%) of Au and Pd was selected based on preliminary catalyst preparation tests and an analysis of the metal content (wt%) by XRF. However, for Pd, the required nominal amount was higher than the targeted amount because the success of Pd deposition was only around ca. 80–90%, whereas the success of Au deposition was ca. 100%. Monometallic Au and Pd catalysts were prepared with a targeted active metal weight percentage of 0.6 wt% on TiO₂ (to be referred to as 0.6Au and 0.6Pd). The bimetallic catalysts were prepared with a targeted active metal weight percentage of 0.3 wt% of Au and 0.3 wt% of Pd (to be referred to as 0.3Au.0.3Pd) and 0.6 wt% of Au and 0.6 wt% of Pd (to be referred to as 0.6Au.0.6Pd). For reference, a TiO₂ catalyst without an active metal was treated similarly.

The microchannel plates (SS 316L) by Institut für Mikrotechnik Mainz GmbH (IMM) with 13 channels with dimensions of 1000 μm width, 150 μm depth and 75 mm length (Fig. 2) were first pretreated in order to enhance the adhesion. The plates were cleaned with a 0.25 wt% citric acid solution in an ultrasound bath for 1 h and thermally oxidized under an ambient air flow at 800 $^{\circ}\text{C}$ for 2 h (ramp 5 $^{\circ}\text{C}/\text{min}$).

The coating procedure for the plates was adopted from the literature [34]. A schematic illustration of the suspension method that was used is provided in Fig. 1. First, PVA (weight-average molecular weight, $M_w = 195\,000\text{ g mol}^{-1}$, Aldrich) was diluted in distilled water (90 $^{\circ}\text{C}$, mixing for 2 h), and then the previously dried catalyst powder was added. The temperature was lowered to 65 $^{\circ}\text{C}$ at approximately 1 $^{\circ}\text{C}/\text{min}$. The mixing at 65 $^{\circ}\text{C}$ was continued for 2 h, and then the suspension was mixed at room temperature for 3 days. The mass proportions of the suspension were PVA:water:catalyst 1:19:4. The coating was applied to the plate by filling the channels with the freshly made suspension and wiping the excess off. The plates were dried at room temperature overnight and calcined under ambient air flow at 450 $^{\circ}\text{C}$ for 2 h (ramp 2 $^{\circ}\text{C}/\text{min}$). The effect of the calcination step on the removal of PVA was measured via thermogravimetric analysis (TGA) from 30 $^{\circ}\text{C}$ to 700 $^{\circ}\text{C}$ in a N_2 atmosphere for the 0.6 wt% Au/TiO₂ catalyst. The final amount of catalyst was 60 \pm 4 mg on two coated plates, i.e., in one structured microreactor.

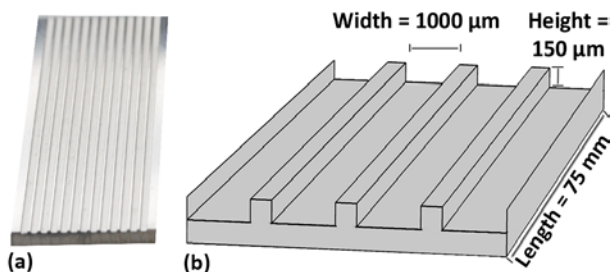


Fig. 2. (a) Photograph of an uncoated microreactor plate, (b) schematic representation of the microchannel plate (note: scale exaggerated for clarity). One microreactor is obtained by connecting two plates with the channels facing each other.

2.2 Characterization of the catalyst powders and the coated plates

Various methods were used to characterize the textural and physical properties and the chemical composition of the catalyst powders and the coated plates. To obtain the coated catalyst powder, the prepared catalyst suspension was coated onto a flat stainless-steel plate. The catalyst powders and the coated plates were calcined under an ambient air flow at 450 $^{\circ}\text{C}$ for 2 h (ramp 2 $^{\circ}\text{C}/\text{min}$) before characterization in order to obtain similar thermal histories. After calcination, the coating was scratched off for analysis.

The surface areas, pore volumes and median pore diameters of the catalyst powders were determined by nitrogen physisorption isotherms at 77 K (Ultra Surfer, Thermo Fischer). The samples were degassed under vacuum for 3 h at 300 $^{\circ}\text{C}$ prior to the measurements. The surface areas were calculated using the Brunauer–Emmett–Teller (BET) method [35], and the pore volumes and pore diameters were calculated using the Barrett–Joyner–Halenda (BJH) method [36] from nitrogen desorption isotherms.

The metal loading of the catalyst powders (coated, calcined and scratched off) was determined via X-ray Fluorescence (XRF) and by Inductively Coupled Plasma Optical Emission Spectroscopy (ICP-OES). The XRF equipment was a wavelength dispersive PANalytical AXIOSmax with an SST-max X-ray source, and the samples were measured as loosely packed powders. For the ICP-OES analysis, the (coated) powders

were first dissolved in a concentrated HCl and HNO₃ mixture, heated at 200 °C for 1 h, cooled down and diluted with distilled water. The equipment used was a Perkin-Elmer DV 7100-ICP-OES.

The effect of coating and calcination on the metal particle sizes and particle size distributions of the active metals was determined for the (i) uncoated and uncalcined catalyst powder, (ii) coated and calcined catalyst powder at 300 °C and (iii) coated and calcined catalyst powder at 450 °C, using a JEOL-2200FS field emission gun (FEG) (scanning) transmission electron microscope (STEM). The elements present on the plate coatings were analyzed with energy dispersive X-ray spectroscopy (EDS).

The thickness of the catalytic coating on the coated plates was measured from sawed-off cross-sections via Scanning Electron Microscopy (SEM) with energy dispersive spectroscopy (SEM-EDS Hitachi S-4700).

2.3 Reactor experiments

The partial oxidation of 1-butanol was studied at atmospheric pressure in a catalyst testing microreactor (CTMR) manufactured and customized to our needs by IMM (Institut für Mikrotechnik Mainz GmbH, Mainz, Germany). The reactor system and assembly materials were 316L grade stainless steel. The reactor system is depicted in Fig. 3. Two coated and calcined plates (450 °C) were placed together face-to-face to create one microchannel reactor (total amount of catalyst = 60±4 mg). 1-Butanol (VWR, 99.9%) was fed with a Gilson 307 pump, evaporated at 125 °C and mixed with the nitrogen flow (AGA, 5.0). Synthetic air (AGA, 5.0) was used as the oxidizing gas for partial oxidation in a stoichiometric ratio. The product gas was analyzed with an online Fourier-transform infrared spectrometer (Gaset instruments CR 5000), and the volumetric flow rate of the dry gas was analyzed by a gas-meter (Ritter). To complement the FT-IR analyses, qualitative and quantitative off-line GC analyses were performed for some gas samples by an Agilent 6890 Series GC with an FID and thermal conductivity detector (TDC).

In an experiment, initially, all the lines to and from the reactor (Fig. 3) were heated to 130 °C in order to avoid condensation of 1-butanol and the products. The inlet line carrying 1-butanol vapors and air to the reactor was kept at 130 °C throughout the experiments, i.e., well above the 1-butanol boiling temperature of 118 °C. As the experiment progressed, the outlet line temperatures were adjusted as follows: i) the 1-butanol vapor and N₂ dilution mixture was passed through the bypass lines (heated to 130 °C) to take the baseline analysis; ii) air was introduced into the mixture passing through the bypass line; iii) the mixture was passed through the reactor; iv) after steady-state activity was achieved at 130 °C (in approximately 1 h), the temperature of the reactor and the outlet lines was increased to 165 °C for the activity measurements. For all the higher temperatures studied, the temperature of the outlet lines was kept at 165 °C and the temperature of the reactor was raised to either 250, 300 or 350 °C. In all the experiments, the partial pressure of 1-butanol was ca. 13.5 kPa and the residence time was 0.137 s. After the experiment, the catalyst was regenerated under a constant synthetic air flow of 100 ml/min at 400 °C for an hour. In all experiments, the carbon balance calculated from the analyzed inlet and outlet gas composition was between 94% and 98%. The experimental error was ± 2 percentage points calculated from 5 repeated experiments.

Conversion of 1-butanol (X) and product yields (Y) were calculated with Equations (1) and (2), respectively:

$$X_{\text{BuOH}} = \frac{\dot{n}_{\text{BuOH,in}} - \dot{n}_{\text{BuOH,out}}}{\dot{n}_{\text{BuOH,in}}} \quad (1)$$

$$Y_i = \frac{\dot{n}_{i,\text{out}}}{\dot{n}_{\text{BuOH,in}}} \quad (2)$$

In the equations, $\dot{n}_{\text{BuOH,in}}$ and $\dot{n}_{\text{BuOH,out}}$ are the molar flows (mol/s) of 1-butanol in the feed and at the outlet of the reactor, respectively, and $\dot{n}_{i,\text{out}}$ is the molar flow (mol/s) of the components exiting the reactor.

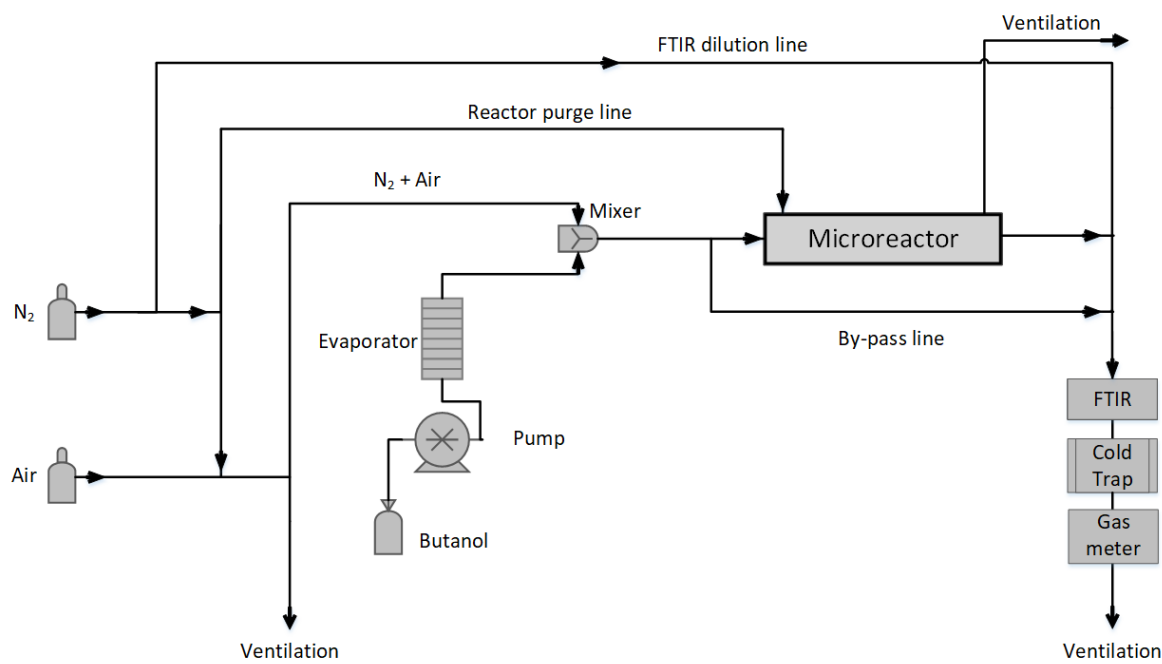


Fig. 3. The experimental setup.

2.4 Stability of the catalyst coatings

The stability of the coated plates was tested as follows: i) using a multistep stress test; ii) using the coated plates in extensive activity tests almost 60 times (each of 6 h duration); iii) storing the coated plates for 6 months (at ambient pressure and temperature) and measuring the activity afterwards to compare to that of fresh catalyst. The stress test consisted of several steps: scratching of the coating, removal of the coating by tape, exposure to pressurized air for 10 s, and dropping the coated plates from 35 cm onto a laminated table. The weight of the coated plates was measured before and after each step.

3. Results

3.1 Characterization of catalyst powders

The BET surface areas, total pore volumes and median pore diameters of all the catalysts, including the supports, are presented in Table 1. The results were the same within $\pm 5\%$. Therefore, the addition of gold and palladium to TiO_2 did not affect the BET surface area, total pore volume or the average pore diameter of the materials.

Table 1. Surface areas, total pore volumes and median pore diameters of the catalyst powders (noble metals on TiO_2 support) from physisorption measurements.

Catalyst code	BET surface area (m^2/g)	Total pore volume (cm^3/g)	Median pore diameter (nm)
TiO_2	53	0.21	16
0.6Au	53	0.25	16
0.6Pd	54	0.25	17
0.3Au0.3Pd	51	0.23	18
0.6Au0.6Pd	50	0.23	18

The amounts of metal in the prepared mono- and bimetallic Au-Pd NPs over TiO_2 coatings were analyzed by XRF and ICP-OES and are presented in Table 2. The targeted amounts differ from the nominal amounts in the case of Pd, where a higher nominal amount of Pd was required to achieve the targeted amount based on preliminary catalyst preparation and metal analysis. Thus, the average success was ca. 100% for Au and ca. 90% (ICP-OES) and ca. 80% (XRF) for Pd based on the nominal active metal added (wt%). Similarly prepared Au-Pd was reported in the literature to have an almost 100% deposition of both of these metals [20]. Therefore, our preparation method still needs more optimization for the deposition of Pd.

Table 2. Metal contents of the catalyst powders: targeted and analyzed by XRF and ICP-OES

Catalyst code	Au (wt%)			Pd (wt%)		
	targeted	XRF	ICP-OES	targeted	XRF	ICP-OES
TiO_2	-	0.0	n.a.	-	0.0	n.a.
0.6Au	0.60	0.6	0.58	-	0	0
0.6Pd	-	0	0	0.60	0.6	0.70
0.3Au0.3Pd	0.30	0.3	0.29	0.30	0.3	0.39
0.6Au0.6Pd	0.60	0.6	n.a.	0.60	0.6	n.a.

n.a. Not analyzed

3.2 Characterization of the catalyst-coated microreactor plates

To analyze the metal particle sizes by TEM, the coating was scratched off of the coated plates after calcination. First, the effect of coating and calcination on the metal particle size distribution for the 0.6Au catalyst was studied. TEM bright field images (shown for the 0.6Au catalyst in Fig. 4 b) were used to determine the particle size distribution of the metals (Fig. 4 a). The coating procedure and subsequent calcination increased the size of the Au NPs. The average metal particle size of the uncoated and uncalcined catalyst powder was 1.8 nm. Coating and calcination at 300 °C increased the average metal particle size to 2.5 nm, and calcination at 450 °C increased the average size further to 3.6 nm. The increase in particle size is likely caused by the exposure to elevated temperatures, in accordance with findings by Comotti et al. [37], who reported that the particle sizes of Au NPs over a TiO₂ support increased from 3.0 nm (uncalcined) to 4.9 nm (after calcination at 550 °C). Since the activity experiments (Section 3.3) were only performed up to 350 °C, the average particle size of gold is not expected to increase during the activity tests. Furthermore, PVA capping can be detected in TEM bright field images [21], but no PVA capping around the Au nanoparticles was detected in the studied catalysts. Moreover, the removal of PVA during the calcination step was confirmed by TGA (not shown).

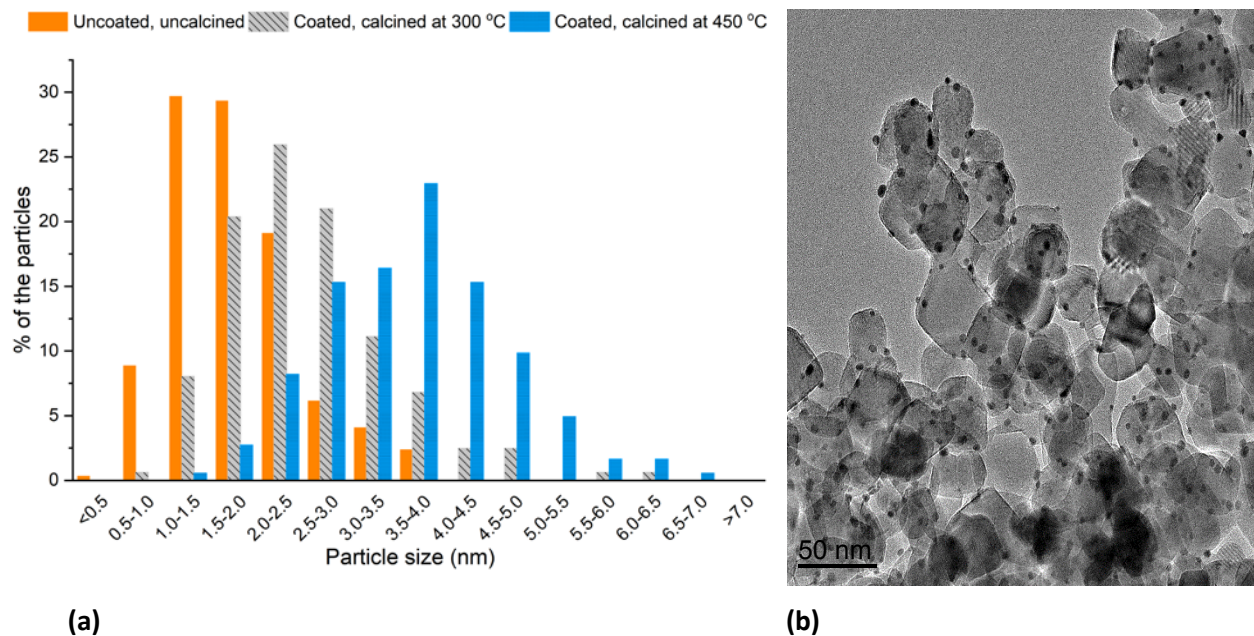


Fig. 4. (a) Effect of calcination and coating on the gold particle size distribution for the 0.6Au catalyst. (b) Representative TEM image of the 0.6Au catalyst coated and calcined at 450 °C, showing Au nanoparticles on the TiO₂ support particles.

The metal particle size distribution of the 0.6Au and 0.3Au0.3Pd catalyst-coated plates after calcination at 450 °C are shown in Fig. 5. For the bimetallic catalysts, the given metal particle sizes are the combined sizes of the Au and Pd nanoparticles. The metal particle size distribution of these catalysts was rather similar. The average metal particle size was 3.6 nm for the gold catalyst and 3.5 nm for the bimetallic catalyst. The metal dispersion for both the catalysts was ca. 35%, assuming a spherical geometry [38]. Furthermore, almost 90% of the particles were within the targeted range of 2-5 nm for both catalysts, which shows that the particle sizes are within the region where gold is expected to be the most catalytically active [18]. For comparison, the average particle sizes of catalysts prepared by Dimitratos et al. [23] via a similar preparation method were 4.6 nm for 1% Au/TiO₂ and 4 nm for 0.5% Au-0.5% Pd catalysts.

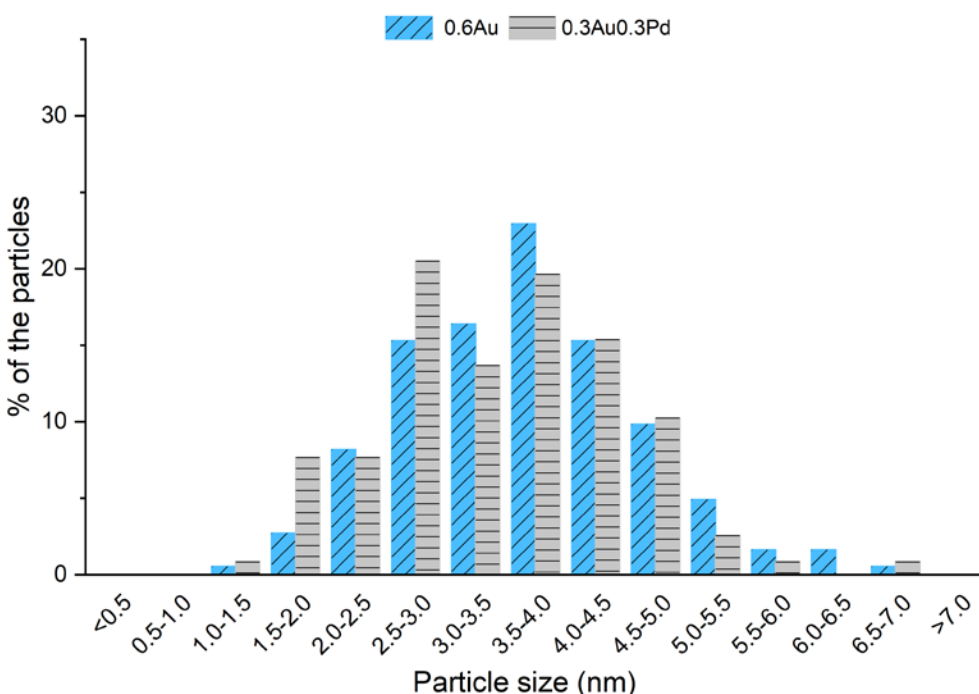


Fig. 5. Metal particle size distribution of the 0.6Au and 0.3Au0.3Pd catalysts coated and calcined at 450 °C.

The composition of the NPs was analyzed during TEM imaging using energy dispersive X-ray spectroscopy (EDS) for the bimetallic 0.3Au0.3Pd catalyst after calcination at 450 °C (Fig. 6). The qualitative EDS analysis showed the presence of individual Au, Pd and titania nanoparticles. Au and Pd appeared to be distributed randomly on the catalyst surface. In addition, the presence of mixed Au-Pd NPs was detected (Fig. 6 c). However, the sampling was not large enough for a statistical analysis. The ratio of Au and Pd in the mixed nanoparticles was approximately 1:1 wt%/wt%.

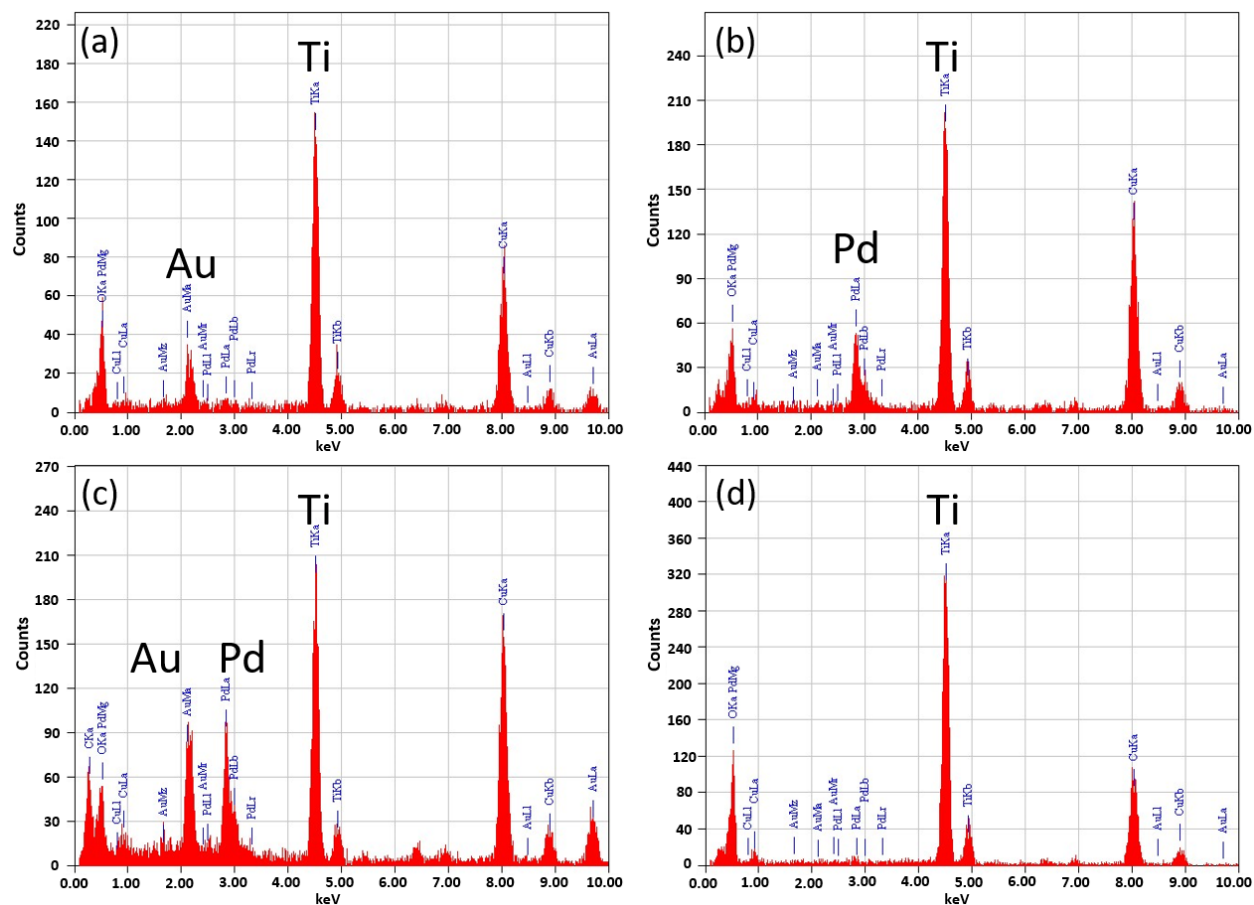
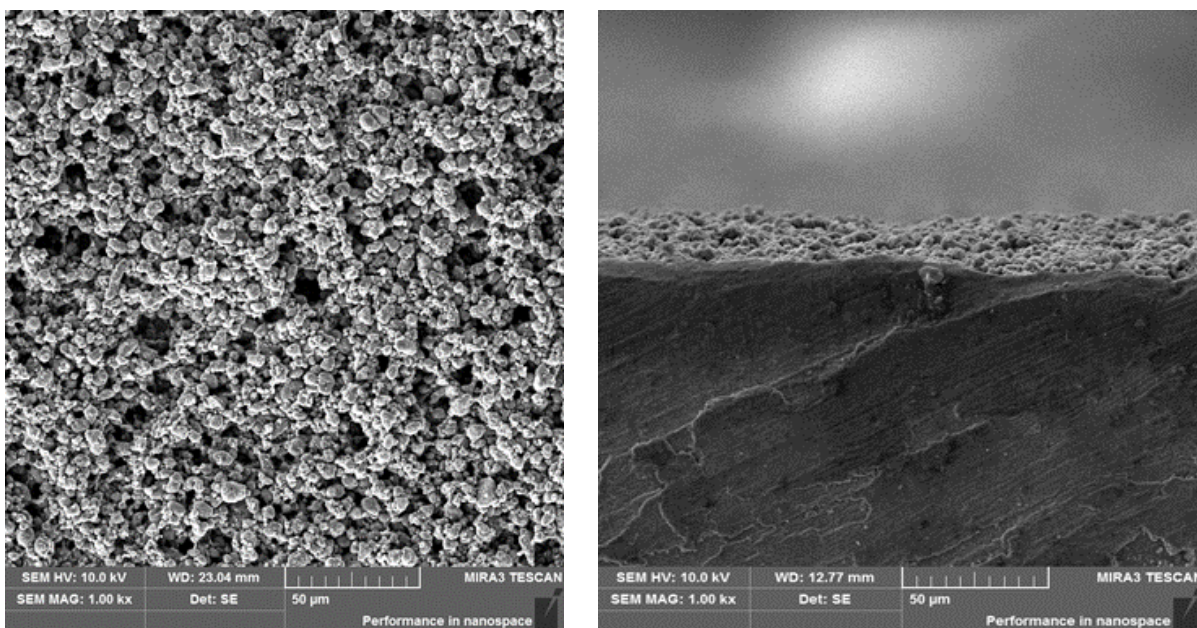


Fig. 6. Representative EDS scans of the metal nanoparticles from the TEM images for the 0.3Au0.3Pd catalyst: (a) Au NPs, (b) Pd NPs, (c) Au-Pd NPs and (d) titania NPs.

The SEM results are presented in Fig. 7 for the 0.6Au catalyst-coated plate. In Fig. 7 a, the coating is shown from the top and in Fig. 7 b, a sawed-off cross-sectional image of a channel is shown. The top view (Fig. 7 a) is a representative image indicating the formation of a uniform porous catalyst layer across all channels. The cross-section shows the thickness of the coating on top of the metal plate (Fig. 7 b). The average thickness of the 13 channels was measured to be $17 \pm 7 \mu\text{m}$. This variation in the coating thickness arises from the plate structure and is a common observation in coating processes [39].



(a)

(b)

Fig. 7. Representative SEM images of the 0.6Au catalyst-coated plate; (a) top view, (b) sawed-off cross-section of a channel.

3.3 Activity tests for 1-butanol partial oxidation

The partial oxidation of 1-butanol was studied with a stoichiometric ratio of 1-butanol and oxygen in the gas phase over TiO_2 , 0.6Au, 0.6Pd, 0.3Au0.3Pd and 0.6Au0.6Pd catalyst-coated microstructured plates, as well as over a blank plate without any coating. In the noncatalytic reference experiments, when the 1-butanol/ N_2 /air mixture was passed through the bypass line (heated to 130 °C), some oxidation reaction products, such as *n*-butyraldehyde, were observed in trace amounts, and the conversion of 1-butanol was low (< 5%).

The conversions of 1-butanol and yields of *n*-butyraldehyde as a function of reaction temperature for all the studied catalysts are shown in Fig. 8. For all the catalysts, the conversion (Fig. 8 a) increased with increasing temperature. The Pd containing mono- (0.6Pd) and bimetallic catalysts (0.3Au0.3Pd and 0.6Au0.6Pd) showed higher conversions compared to the monometallic Au catalyst (0.6Au). At 350 °C, both the monometallic 0.6Au and 0.6Pd catalysts showed similar conversions of ca. 64%. The conversion with the bimetallic (0.3Au0.3Pd and 0.6Au0.6Pd) catalysts at 350 °C was 5–10% higher than that with the monometallic 0.6Au and 0.6Pd catalysts. The TiO_2 catalyst and blank plates showed similar conversions, indicating that the activity of TiO_2 was low.

The *n*-butyraldehyde yields with increasing temperature showed varying trends with the insertion of different metal(s) on the titania support (Fig. 8b). For the TiO_2 coated and uncoated microreactor plates

(blank), the yield of *n*-butyraldehyde increased with increasing temperature, and the highest yield was achieved at 350 °C (approximately 16-20%). The incorporation of 0.6 wt% of gold on the TiO₂ support decreased the temperature required for a 15% yield to 250 °C, and a maximum yield of 20% was obtained at 300 °C. For all the Pd-containing catalysts (0.6Pd, 0.3Au0.3Pd and 0.6Au0.6Pd), the highest yield of *n*-butyraldehyde was achieved at 350 °C but was below 10%. Thus, the incorporation of gold onto a TiO₂ support favored the formation of *n*-butyraldehyde from 250 to 300 °C.

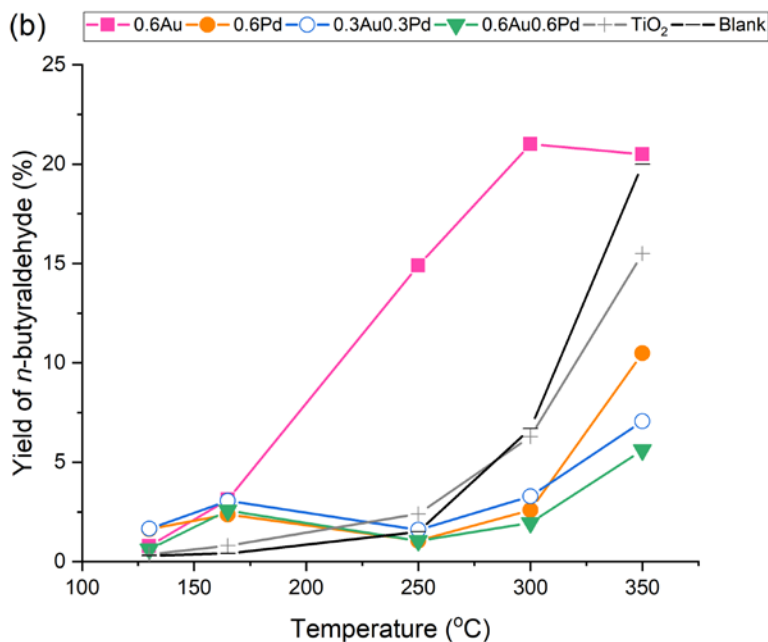
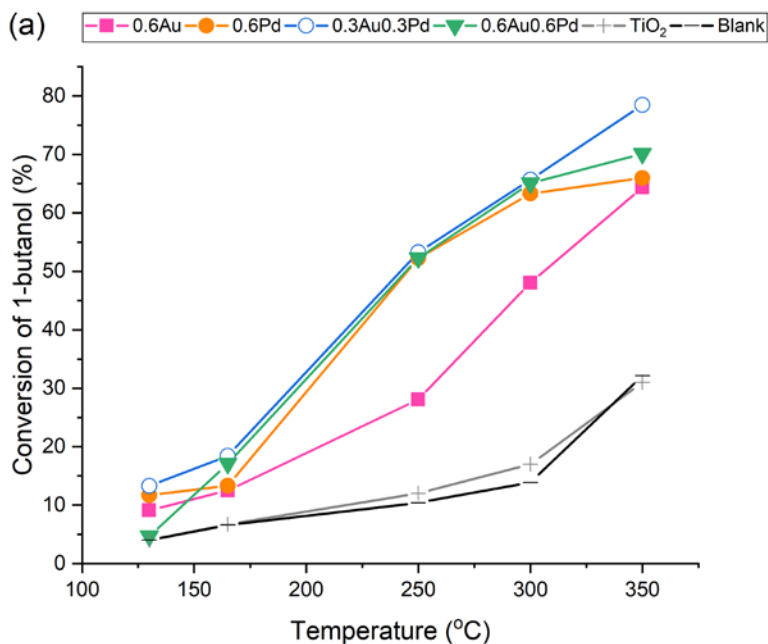


Fig. 8. Conversion of 1-butanol (a) and yields of *n*-butyraldehyde (b) over the studied catalysts, TiO₂ (+), 0.6Au (■), 0.6Pd (●), 0.3Au0.3Pd (○), and 0.6Au0.6Pd (▼), and blank plates (-). The 1-butanol partial pressure was 13.5 kPa with a residence time of 0.137 s.

The main products for all the catalysts were *n*-butyraldehyde, water, CO, CO₂, butenes and propene. The yields of all the main products are shown in Fig. 9 for the studied metal catalysts at 250 °C. Other products observed in trace amounts included *n*-butylbutyrate, 4-heptanone and *n*-butanoic acid. The highest yield of *n*-butyraldehyde (ca. 15%) was measured with the 0.6Au catalyst. The Pd-containing catalysts (0.6Pd, 0.3Au0.3Pd and 0.6Au0.6Pd) showed good activity but poor yield of *n*-butyraldehyde and favored the formation of CO, CO₂ and propene. The TiO₂-coated and uncoated microreactor plates favored *n*-butyraldehyde formation, likely due to thermal reactions. In addition to the aforementioned products, traces of dehydration and thermal degradation products, such as dibutyl ether, propane and C₄H₁₀, were also observed with all studied catalysts. Furthermore, the off-line GC analysis showed the presence of H₂.

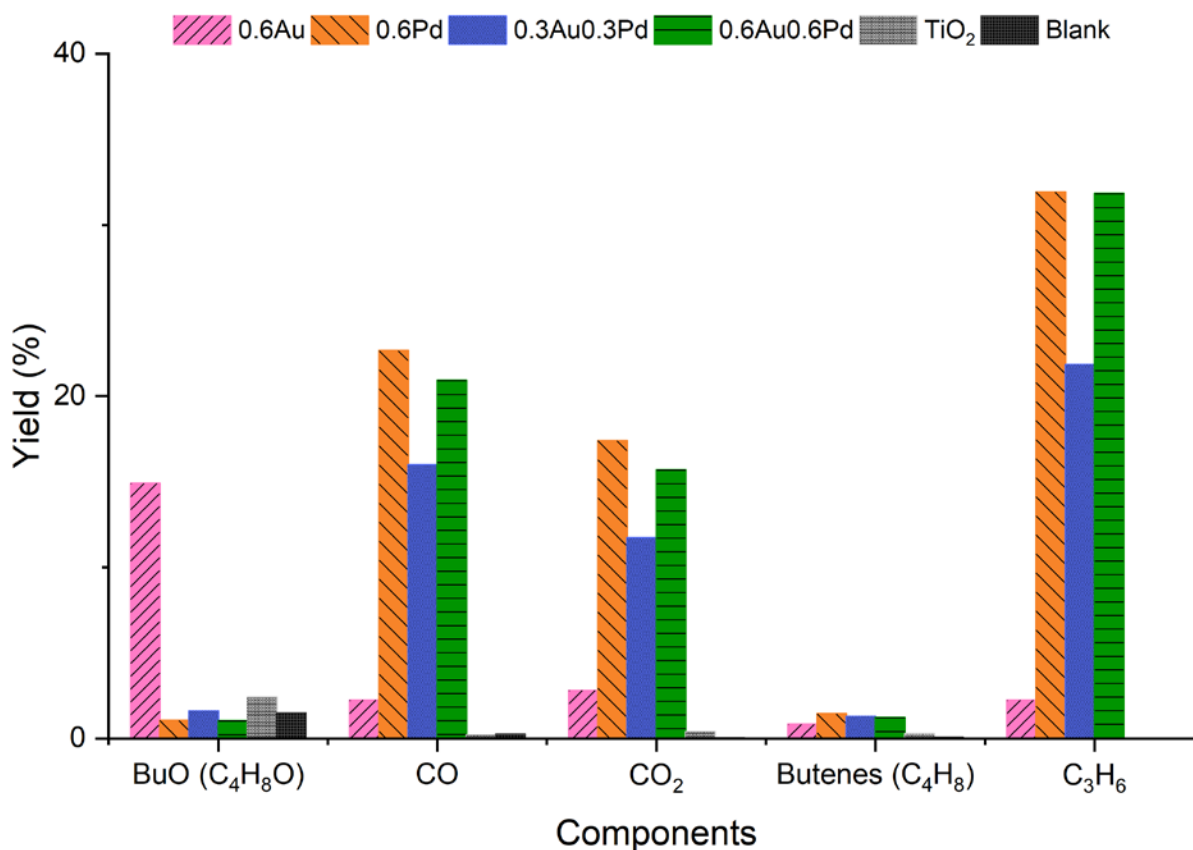
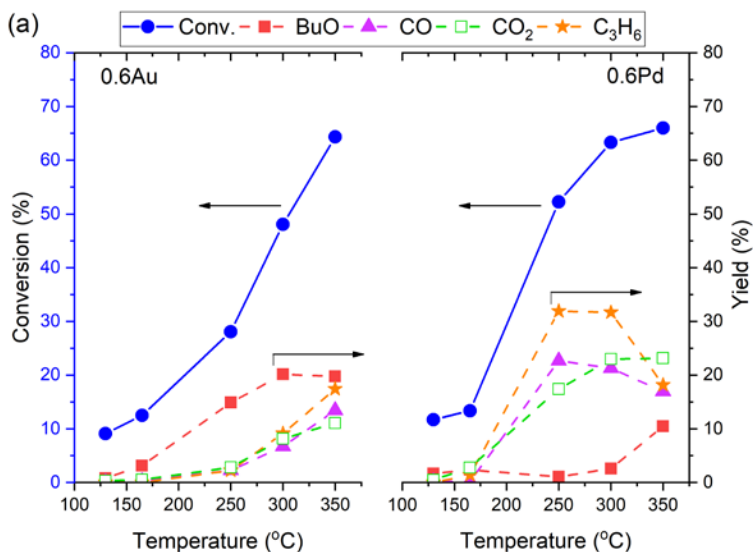


Fig. 9. Yields of the main products, *n*-butyraldehyde (BuO), carbon monoxide, carbon dioxide, butenes and propene, using the studied catalysts at 250 °C with a 1-butanol partial pressure of 13.5 kPa and residence time of 0.137 s.

The incorporation of palladium into the catalysts increased the yield of propene as the yield of *n*-butyraldehyde decreased from 165 to 250 °C (Fig. 10). Using the TiO₂ support and the 0.6Au catalyst, the yield of CO, CO₂ and propene increased with increasing temperature. However, with the palladium-containing catalysts, the yield of CO and propene first increased, reached a maximum, and then started to decrease with increasing temperature. Thus, the product distribution trends were very different for the 0.6Au and Pd-containing catalysts. The CO₂ yield increased or remained stable for all the catalysts. The yield of propene was nearly the same as that of CO with the 0.6Au catalyst and the TiO₂ support throughout the studied temperature range. For the Pd-containing catalysts, the yield of propene was higher than that of CO, but the trends with increasing temperature were similar.



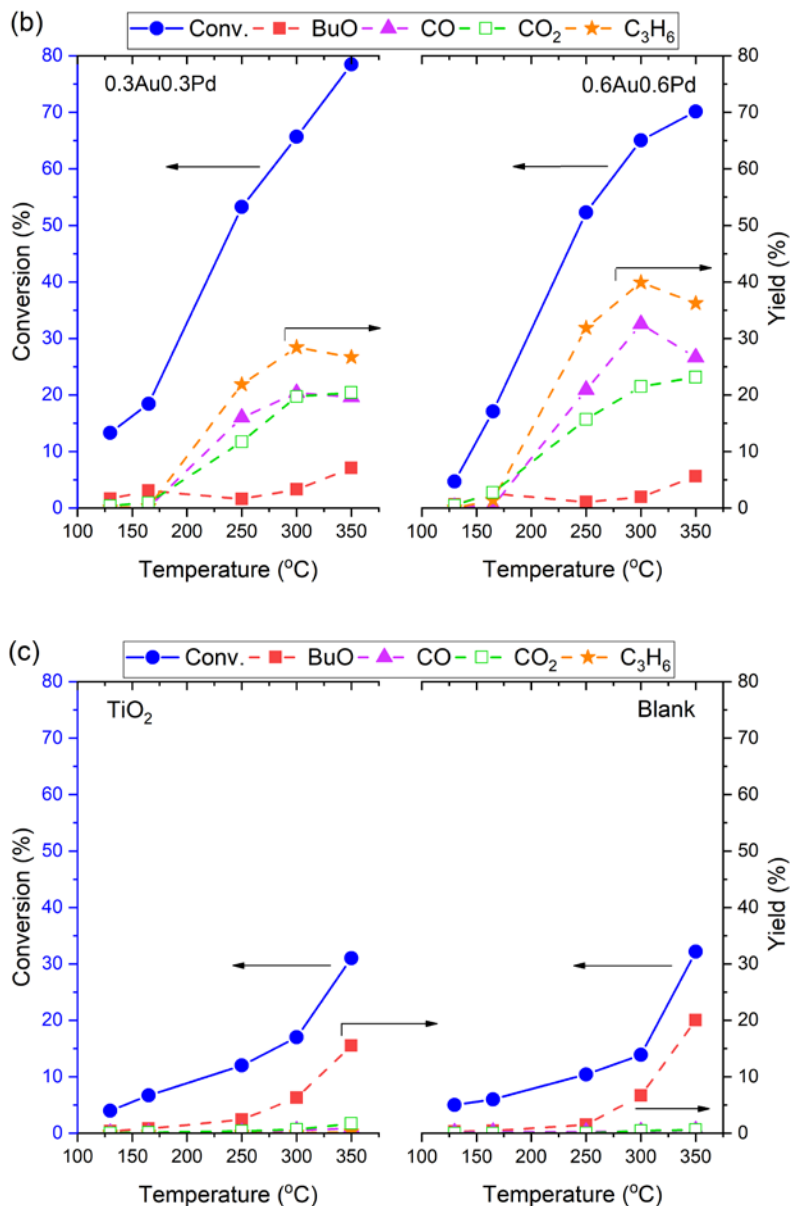


Fig. 10. Conversions (solid lines) and yields (dotted lines) during 1-butanol partial oxidation over the coated catalysts at 250 °C with a 1-butanol partial pressure of 13.5 kPa and residence time of 0.137 s; (a) comparison of the 0.6Au and 0.6Pd catalysts, (b) comparison of the bimetallic 0.3Au0.3Pd and 0.6Au0.6Pd catalysts, and (c) comparison of TiO₂-coated catalyst and uncoated plate (blank).

3.4 Stability, reusability and in situ regeneration of the 0.6Au catalyst-coated plates

The stability of the coatings was analyzed using a multistep stress test that included scratching and dropping the coated plates. The overall weight loss in the stress test was less than 1% for the studied catalysts. Thus, the catalyst coatings showed good adhesion.

The catalytic activity of the coated plates was measured repeatedly (almost 60 times) for one pair of 0.6Au catalyst plates. Regeneration of the catalyst was performed in situ with a synthetic air flow at 400 °C for 1 h. The results for the 1st and 57th runs are shown in Table 3. In addition, the stability of the coated plates stored at ambient conditions for 6 months is shown in Table 3. The conversion of 1-butanol and yields of the main components were the same within experimental error between the fresh, stored and repeatedly used coated plates at each temperature. Thus, the catalytic activity of the 0.6Au catalyst-coated plates was maintained throughout these experiments, indicating the high stability of the coating, as well as its excellent durability and reusability. During the in situ regeneration step, a small amount of CO₂ (approximately 0.5% of fed carbon atoms) was detected, indicating that some carbonaceous species had formed on the catalyst or in the lines. However, for comparison, recycling up to five times has been previously reported for supported Au NPs using an ex situ regeneration of the catalyst via centrifugation and washing [40]. Therefore, the reusability of these catalyst-coated microreactor plates seems outstanding.

Table 3. Conversion of 1-butanol over the fresh, stored (6 months) and repeatedly used 0.6Au catalyst plates.

Temperature (°C)	Conversion of 1-butanol (%)		
	Fresh (1 st run)	After storage	After 57 th run
130	11	9	9
165	14	10	14
250	28	27	28
300	44	46	46
350	67	66	64

4. Discussion

4.1 Au and Pd NPs supported on TiO₂ catalysts: preparation, characterization and coating

To achieve a narrow particle size distribution and small NPs, a colloidal preparation method was chosen, more precisely, the sol-immobilization of NPs using polyvinyl alcohol (PVA) as the stabilizing agent. Although this preparation method is well-known to yield excellent powder catalysts [41], before this work, it was not known how these NPs would perform in a coating procedure. The coating and calcination of the coated plates increased the average metal particle size from 1.8 nm to 3.6 nm for the 0.6Au catalyst (Fig. 4). The metal particle size distributions of the coated and calcined (at 450 °C) 0.6Au and 0.3Au0.3Pd catalysts were rather similar (Fig. 5), as well as their average metal particle sizes (3.6 nm for the 0.6Au catalyst and 3.5 nm for the 0.3Au0.3Pd catalyst), suggesting that both the gold and palladium nanoparticles were well-dispersed after the coating process. Au NPs supported on titania have been found to be the most active in this particle size range [42], which has been related to electron transfer between the Au particles and TiO₂ support [31]. Pritchard et al. [43] studied the effect of calcination temperature on a 0.5% Au – 0.5% Pd catalyst prepared by a sol-immobilization method and

showed that after calcination at 400 °C, the mean particle size was 6.0 nm. As PVA capping was not detected around the metal nanoparticles (Section 3.2), the low agglomeration of the nanoparticles observed in this work (average particle size of 3.6 nm after calcination at 450 °C) is believed to be caused by the strong interactions between the nanoparticles and the titania support, in accordance with the findings of Pritchard et al. [43].

The simultaneous introduction of Au and Pd in the preparation of catalysts by a sol-immobilization method has been shown by Peneau et al. [44] to result in homogeneous Au-Pd alloys, whereas core-shell structures were observed after sequential introduction of the metals [44]. Furthermore, it has been demonstrated that after exposing an Au-Pd catalyst (simultaneous introduction of metals) to calcination at 400 °C, all the metal particles remained as random Au-Pd alloys [45]. Therefore, in the present study, the observed mixture of Au-Pd NPs in the bimetallic catalyst probably contained Au-Pd alloys in addition to individual Au and Pd NPs.

The thickness of the catalyst coating has been reported to be the most significant parameter related to limitations in internal diffusion [9]. A thin layer of the catalyst is necessary in order to avoid internal mass transfer resistance and to operate the catalyst-coated microreactors in the desired kinetic regime [10,46]. According to related studies, the thickness of the catalyst coating should be less than 40 µm, based on empirical correlation [10,11], which contributes to shorter characteristic diffusion time scales [39]. The catalyst coating layer thickness in this study was 17±7 µm. Thus, it can be concluded that the 1-butanol partial oxidation experiments were likely performed within the kinetic regime.

4.2 Au and Pd NPs supported on TiO₂ catalysts: activity and reaction pathways

The most significant result was the performance of the 0.6Au-coated catalyst plates, which demonstrated the highest yield (Figs. 8 b and 9) of *n*-butyraldehyde among the studied catalysts. The yield of *n*-butyraldehyde was approximately 15% at 250 °C and approximately 20% at 300 °C using the 0.6Au catalyst. The yield was slightly lower at 350 °C than at 300 °C, due to an increased yield of CO, CO₂ and propene (Fig. 10). Therefore, the operation temperature should not exceed 300 °C when using the 0.6Au catalyst. Tuning the yield of aldehyde from the primary alcohol using Au NPs has been reported to be challenging and often results in the formation of acids rather than aldehydes [18]. Thus, the prepared 0.6 wt% Au/TiO₂ catalyst demonstrated both reasonable activity and a reasonable yield of *n*-butyraldehyde.

A general reaction scheme for the catalytic partial oxidation of 1-butanol in the gas phase is proposed in Fig. 11. The desired main reaction is the oxidative dehydrogenation of 1-butanol to *n*-butyraldehyde (1). The dehydrogenation of 1-butanol also leads to *n*-butyraldehyde (2). In addition, undesired reactions such as the dehydration of 1-butanol to butenes (3), decarbonylation of *n*-butyraldehyde to CO and propane (4), reversible dehydrogenation of propane to propene (5), reversible retro-hydroformylation reaction of *n*-butyraldehyde to propene, CO and H₂ (6), and total oxidation of 1-butanol (7) and *n*-butyraldehyde (8) and oxidation of CO to CO₂ (9) can take place. For all the catalysts, the simultaneous formation of *n*-butyraldehyde and H₂O is believed to be caused by oxidative dehydrogenation (ODH) of 1-butanol following a Mars-van Krevelen mechanism, as was suggested by Holz et al. [27] for the partial oxidation of ethanol in the gas phase over TiO₂. Comparing the activity of Au/TiO₂ to that of the TiO₂ support in the partial oxidation of 1-butanol (Figs. 8-10), oxidative dehydrogenation is believed to take

place in the interfacial region between the gold nanoparticles and the titania support and involves lattice oxygen. Other products are present in trace amounts, such as dibutylether, 4-heptanone, *n*-butylbutyrate, *n*-butanoic acid and butane, but are not included in the proposed scheme.

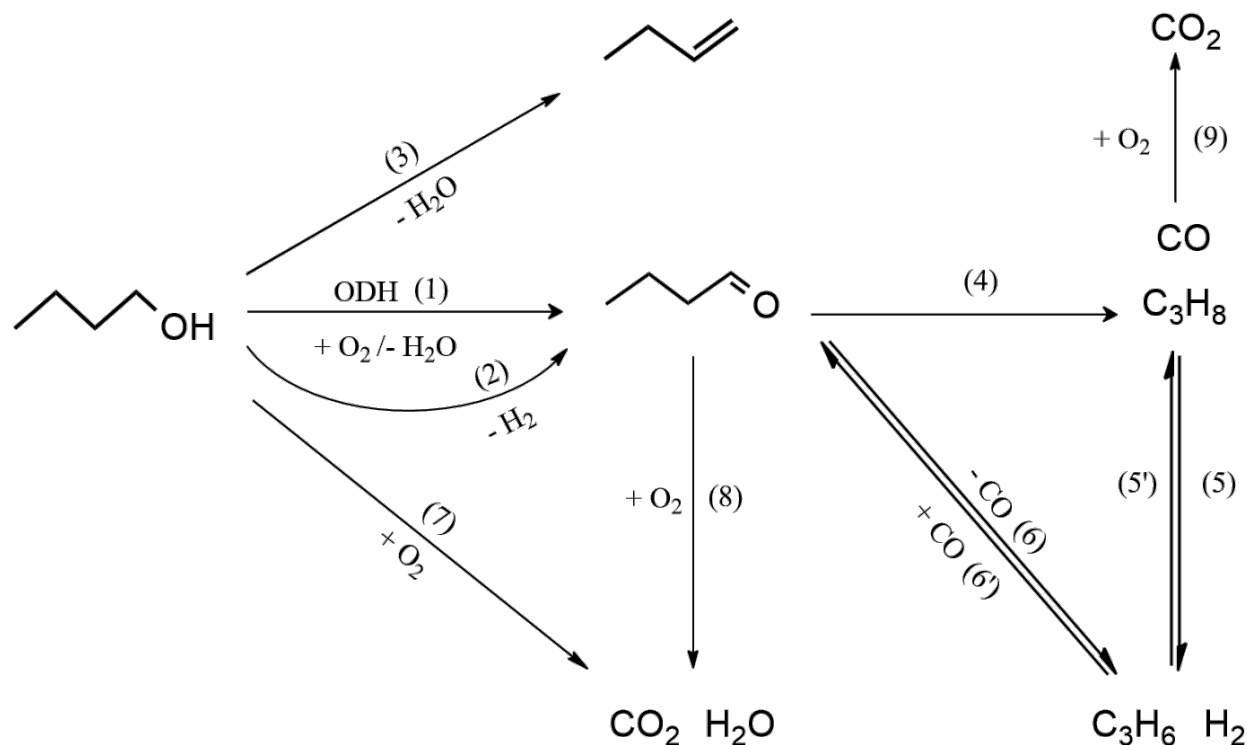


Fig. 11. Proposed reaction scheme for 1-butanol partial oxidation using the studied catalysts.

For all the noble metal catalysts, the simultaneous formation of propene, CO and H_2 suggest that *n*-butyraldehyde undergoes a retro-hydroformylation reaction. The aldehyde retro-hydroformylation reactions were proposed by Kusomoto et al. [47], who performed mechanistic control experiments of aliphatic aldehydes to the corresponding alkenes and synthesis gases with hydroxycyclopentadienyl iridium complexes as the catalysts. They concluded that the reaction proceeded by retro-hydroformylation and not by the sequential decarbonylation–dehydrogenation or dehydrogenation–decarbonylation. In our experiments, the higher amounts of propene and CO (Fig. 9 and 10) suggest that the formation of propene and CO from *n*-butyraldehyde is likely taking place by a retro-hydroformylation reaction (6). Propane could be formed either by hydrogenation of propene (5') or by a decarbonylation reaction (4). Furthermore, as the off-line GC analysis for the blank plates and TiO_2 showed the presence of H_2 , a dehydrogenation reaction of 1-butanol to *n*-butyraldehyde (2) is likely also taking place at higher temperatures. However, further mechanistic studies are needed to clarify the proposed reaction scheme.

Compared to the observations in the liquid phase, the lack of over-oxidized products, i.e., butyric acid, for all the studied catalysts in this work was expected because the reactor was operated in the gas phase. Furthermore, any formed butyric acid could undergo further oxidation to CO_2 , as was proposed by Holz et al. [27] for ethanol partial oxidation over Au/TiO_2 . In the liquid phase, the over-oxidation of *n*-

butyraldehyde to form butyric acid can be prevented only at an intermediate conversion of 1-butanol over Au-Pd/TiO₂ [26]. Biella and Rossi [15] and Requies et al. [17,28] have reported similar observations for the partial oxidation and dehydrogenation of 1-butanol in the gas phase over SiO₂, CeO₂, TiO₂ and ZrO₂ supported Au, Ru and Cu catalysts. The reproducibility of the catalytic activity for the 0.6 wt% Au/TiO₂ catalyst in our study suggests that operated in the gas-phase in the coated microreactor with Au NPs below 5 nm likely suppresses the formation of *n*-butylbutyrate, *n*-butanoic acid, 4-heptanone and dibutylether. In addition, the shorter residence times (milliseconds) with the microreactors assist in the enhanced yield of the desired product when the proper catalyst and reaction conditions are chosen, thus avoiding unwanted intermediates and undesired products.

The presence of small amounts of dehydration products when using all the catalysts can be attributed to the acid-catalyzed dehydration of 1-butanol to form butenes, which takes place on the support as titania (TiO₂) is known to be significantly acidic [48]. Similar observations in the gas phase oxidation of ethanol over Au/TiO₂ were reported by Sobolev et al. [48] and Holz et al. [27]. For all the Pd-containing catalysts, the trend with increasing temperature, 165 °C to 250 °C, showed that as the yield of *n*-butyraldehyde started to decrease, the yield of CO₂ and propene started to increase (Fig. 10). The formed *n*-butyraldehyde can react further (Fig. 11) to form propene, CO and H₂. The offset temperature for the shift in yield of *n*-butyraldehyde was observed to be approximately 300 °C with the 0.6Au catalyst, whereas all the Pd-containing catalysts showed its initiation at approximately 165 °C. The lower yield of CO compared to C₃H₆ (Fig. 10) is caused by the oxidation of CO to CO₂, which is expected as both nano Au and Pd have been reported to be active in CO oxidation, even at lower temperatures [49–51]. For all the Pd-containing catalysts, the yield of *n*-butyraldehyde started to increase with the temperature from 300 °C to 350 °C, whereas the yield of propene and CO started to decrease. This increasing *n*-butyraldehyde yield was similar to the observed trends for the TiO₂ support and blank plates, indicating the formation of *n*-butyraldehyde from thermal reactions.

4.3 Durability and regenerability of the coated plates

The durability and full recovery of catalytic activity (regenerability) of the coated catalyst plates was successfully demonstrated over 57 runs for the 0.6 wt% Au/TiO₂ catalyst. To our knowledge, the highest reported recyclability of Au NP catalysts in the literature is five cycles [18]. Mahyari et al. [40] have reported the stable activity of Au NPs supported on supramolecular ionic-liquid-grafted graphene for benzyl alcohol oxidation in 1 h on a stream up to five times via filtration, washing and reuse of the catalyst. The catalyst recyclability/reusability using microreactors in this work arises from the mechanical robustness of the coated catalyst and from the stable activity and the ease of their regeneration. We have successfully demonstrated the advantages of using the characteristic microreactor flow and heat transfer properties to enhance the yield of the desired product, i.e., *n*-butyraldehyde, in combination with using a low metal loading for Au NPs in the coated catalyst.

5. Conclusions

Partial oxidation of 1-butanol to *n*-butyraldehyde was studied in the gas phase at 130–350 °C using coated catalysts in a structured catalyst testing microreactor. The coated catalysts consisted of TiO₂-supported mono- and bimetallic gold and palladium catalysts, which were prepared by a sol-immobilization method. Coating the catalytic powders on the microreactor plates yielded mechanically and catalytically stable plates with narrow particle size distributions (<5 nm) of the metal(s) and small average particle sizes (ca. 3.6 nm), even after calcination at 450 °C. Furthermore, the coating was sufficiently thin (17±7 μm), such that the microreactor could be operated within the desired kinetic regime.

The TiO₂-coated plates showed the similar conversion of 1-butanol to uncoated stainless-steel plates, indicating the negligible activity of the TiO₂ support. The incorporation of Au and Pd (0.3-0.6 wt%) increased the conversion of 1-butanol between 130 °C and 350 °C. The highest conversion of 1-butanol throughout the studied temperature range was achieved over the bimetallic 0.3Au0.3Pd catalyst-coated plates, with a maximum of ca. 80% at 350 °C. However, the highest yield of *n*-butyraldehyde throughout the studied temperature range was detected using the 0.6 wt% Au/TiO₂ catalyst-coated plates, whereas the presence of Pd resulted in higher yield of C₃H₆, CO and CO₂. A significant finding was that butanoic acid was only present in trace amounts for all the studied catalysts. The main reason for this is likely that the operation was performed in the gas phase with a flow-through reactor, and the shorter residence times (milliseconds) in the microreactors seem to limit further oxidation of *n*-butyraldehyde to *n*-butanoic acid.

In conclusion, the Au/TiO₂ (0.6 wt%) catalyst showed the best yield of *n*-butyraldehyde; moreover, the catalyst coating on the microreactor plates showed outstanding durability and reusability (stable activity in 57 experiments) with in situ regeneration. To improve the yield using the Au/TiO₂ catalyst, the catalyst preparation method could be further optimized in the future studies.

Acknowledgments

The Academy of Finland MICATOX project is acknowledged for funding this work. Giovanni Marin is thanked for the XRF-analysis, Hannu Revitzer for the ICP-OES-analysis, Eveliina Mäkelä for the physisorption measurements, Suvi Nummipuro for assistance in catalyst preparation, Janne-Joonas Tiitinen for assistance in running experiments, Hua Jing for TEM images and Eero Haimi for SEM images at Aalto University. Professor Tapio Salmi and his team are thanked for their valuable discussions on 1-butanol oxidation reactions. The Bioeconomy Infrastructure and Nanomicroscopy Center (Aalto-NMC) at Aalto University were used to complete the work.

5. References

- [1] V. Hessel, S. Hardt, H. Löwe, Chemical Micro Process Engineering, Wiley-VCH Weinheim, 2004.
- [2] F.J. Keil, Modeling of Process Intensification, Wiley-VCH Weinheim, 2007.
- [3] B. Gutmann, D. Cantillo, C.O. Kappe, Angew. Chemie - Int. Ed. 54 (2015) 6688–6728.
- [4] F. Fanelli, G. Parisi, L. Degennaro, R. Luisi, Beilstein J. Org. Chem. 13 (2017) 520–542.

- [5] S. Walter, S. Malmberg, B. Schmidt, M.A. Liauw, *Catal. Today* 110 (2005) 15–25.
- [6] G. Kolb, V. Hessel, *Chem. Eng. J.* 98 (2004) 1–38.
- [7] L. Kiwi-Minsker, A. Renken, *Catal. Today* 110 (2005) 2–14.
- [8] K. Haas-Santo, O. Görke, P. Pfeifer, K. Schubert, *Chim. Int. J. Chem.* 56 (2002) 605–610.
- [9] W. Reschetilowski, *Microreactors in Preparative Chemistry*, Wiley-VCH Verlag GmbH and Co.KGaA, Weinheim, Germany., 2013.
- [10] S.A. Schmidt, Q. Balme, N. Gemo, N. Kumar, K. Eränen, D.Y. Murzin, T. Salmi, *Chem. Eng. Sci.* 134 (2015) 681–693.
- [11] Y. Khan, M. Marin, R. Karinen, J. Lehtonen, J. Kanervo, *Chem. Eng. Sci.* 137 (2015) 740–751.
- [12] C. Chen, L. Wang, G. Xiao, Y. Liu, Z. Xiao, Q. Deng, P. Yao, *Bioresour. Technol.* 163 (2014) 6–11.
- [13] G. Jurgens, S. Survase, O. Berezina, E. Sklavounos, J. Linnekoski, A. Kurkijärvi, M. Väkevä, A. van Heiningen, T. Granström, *Biotechnol. Lett.* 34 (2012) 1415–1434.
- [14] M. Mascal, *Biofuels*, *Bioprod. Bioref.* 6 (2012) 483–493.
- [15] S. Biella, M. Rossi, *Chem. Commun.* 3 (2003) 378–379.
- [16] H. Bahrmann, H. Bach, *Ullmann’s Encyclopedia of Industrial Chemistry: Oxo Synthesis*, 7th ed., Wiley-VCH Verlag GmbH & Co. KGaA, 2005.
- [17] J. Requies, M.B. Güemez, A. Iriondo, V.L. Barrio, J.F. Cambra, P.L. Arias, *Catal. Letters* 142 (2012) 417–426.
- [18] A.S. Sharma, H. Kaur, D. Shah, *RSC Adv.* 6 (2016) 28688–28727.
- [19] M. Haruta, *Chem. Rec.* 3 (2003) 75–87.
- [20] I. Gandarias, P.J. Miedziak, E. Nowicka, M. Douthwaite, D.J. Morgan, G.J. Hutchings, S.H. Taylor, *ChemSusChem* 8 (2015) 473–480.
- [21] A. Villa, D. Wang, D. Sheng, S. Cd, L. Prati, *Catal. Sci. Technol* 5 (2015) 3036–3041.
- [22] J.A. Lopez-Sanchez, N. Dimitratos, P. Miedziak, E. Ntainjua, J.K. Edwards, D. Morgan, A.F. Carley, R. Tiruvalam, C.J. Kiely, G.J. Hutchings, *Phys. Chem. Chem. Phys.* 10 (2008) 1921–1930.
- [23] N. Dimitratos, J.A. Lopez-Sanchez, J.M. Anthonykutti, G. Brett, A.F. Carley, R.C. Tiruvalam, A. a Herzing, C.J. Kiely, D.W. Knight, G.J. Hutchings, *Phys. Chem. Chem. Phys.* 11 (2009) 4952–4961.
- [24] C. Louis, *Catalysts* 6 (2016) 110–137.
- [25] M. Signoretto, F.F. Menegazzo, A. Di Michele, E. Fioriniello, *Catalysts* 6 (2016) 87.
- [26] I. Gandarias, E. Nowicka, B.J. May, S. Alghareed, R.D. Armstrong, P.J. Miedziak, S.H. Taylor, *Catal. Sci. Technol.* 6 (2016) 4201–4209.
- [27] M.C. Holz, K. Tölle, M. Muhler, *Catal. Sci. Technol.* 4 (2014) 3495–3504.
- [28] J. Requies, M.B. Güemez, P. Maireles, A. Iriondo, V.L. Barrio, J.F. Cambra, P.L. Arias, *Appl. Catal. A Gen.* 423–424 (2012) 185–191.

- [29] S.J. Tauster, *Acc. Chem. Res.* 20 (1987) 389–394.
- [30] C.J. Pan, M.C. Tsai, W.N. Su, J. Rick, N.G. Akalework, A.K. Agegnehu, S.Y. Cheng, B.J. Hwang, *J. Taiwan Inst. Chem. Eng.* 74 (2017) 154–186.
- [31] K. Okazaki, S. Ichikawa, Y. Maeda, M. Haruta, M. Kohyama, *Appl. Catal. A Gen.* 291 (2005) 45–54.
- [32] P. Munnik, P.E. De Jongh, K.P. De Jong, *Chem. Rev.* 115 (2015) 6687–6718.
- [33] M. Pelaez, N.T. Nolan, S.C. Pillai, M.K. Seery, P. Falaras, A.G. Kontos, P.S.M. Dunlop, J.W.J. Hamilton, J.A. Byrne, K. O’Shea, M.H. Entezari, D.D. Dionysiou, *Appl. Catal. B Environ.* 125 (2012) 331–349.
- [34] A. Pashkova, L. Greiner, U. Krtischil, C. Hofmann, R. Zapf, *Appl. Catal. A Gen.* 464 (2013) 281–287.
- [35] S. Brunauer, P.H. Emmett, E. Teller, *J. Am. Chem. Soc.* 60 (1938) 309–319.
- [36] E.P. Barrett, L.G. Joyner, P.P. Halenda, *J. Am. Chem. Soc.* 73 (1951) 373–380.
- [37] M. Comotti, W.-C. Li, B. Spliethoff, F. Schüth, *J. Am. Chem. Soc.* 128 (2006) 917–924.
- [38] G. Ertl, H. Knözinger, F. Schüth, J. Weitkamp, *Handbook of Heterogeneous Catalysis*, 2nd ed., Wiley-VCH Verlag GmbH & Co. KGaA, 2008.
- [39] J.A. Moulijn, F. Kapteijn, *Curr. Opin. Chem. Eng.* 2 (2013) 346–353.
- [40] M. Mahyari, A. Shaabani, Y. Bide, *RSC Adv.* 3 (2013) 22509–22517.
- [41] A. Villa, D. Wang, G.M. Veith, F. Vindigni, L. Prati, *Catal. Sci. Technol.* 3 (2013) 3036–3041.
- [42] B. Hvolbæk, T.V.W. Janssens, B.S. Clausen, H. Falsig, C.H. Christensen, J.K. Nørskov, *Nano Today* 2 (2007) 14–18.
- [43] J. Pritchard, M. Piccinini, R. Tiruvalam, Q. He, N. Dimitratos, J.A. Lopez-Sanchez, D.J. Morgan, A.F. Carley, J.K. Edwards, C.J. Kiely, G.J. Hutchings, *Catal. Sci. Technol.* 3 (2013) 308–317.
- [44] V. Peneau, Q. He, G. Shaw, S.A. Kondrat, T.E. Davies, P. Miedziak, M. Forde, N. Dimitratos, C.J. Kiely, G.J. Hutchings, *Phys. Chem. Chem. Phys.* 15 (2013) 10636–10644.
- [45] R.C. Tiruvalam, J.C. Pritchard, N. Dimitratos, J.A. Lopez-Sanchez, J.K. Edwards, A.F. Carley, G.J. Hutchings, C.J. Kiely, *Faraday Discuss.* 152 (2011) 63–86.
- [46] Y. Khan, M. Marin, R. Karinen, J. Lehtonen, *Chem. Eng. Process.* 110 (2016) 97–105.
- [47] S. Kusumoto, T. Tatsuki, K. Nozaki, *Angew. Chemie - Int. Ed.* 54 (2015) 8458–8461.
- [48] V.I. Sobolev, K.Y. Koltunov, O.A. Simakova, A.R. Leino, D.Y. Murzin, *Appl. Catal. A Gen.* 433–434 (2012) 88–95.
- [49] T.V.W. Janssens, B.S. Clausen, B. Hvolbæk, H. Falsig, C.H. Christensen, T. Bligaard, J.K. Nørskov, *Top. Catal.* 44 (2007) 15–26.
- [50] E.J. Peterson, A.T. DeLaRiva, S. Lin, R.S. Johnson, H. Guo, J.T. Miller, J.H. Kwak, C.H.F. Peden, B. Kiefer, L.F. Allard, F.H. Ribeiro, A.K. Datye, *Nat. Commun.* 5 (2014) 1–11.
- [51] M. Haruta, T. Kobayashi, H. Sano, N. Yamada, *Chem. Lett.* 16 (1987) 405–408.